Active noise thin-plate spline smoothing method for full-field strain measurement by digital image correlation

Jiaqing Zhao (赵加清), Pan Zeng (曾 攀)*, Liping Lei(雷丽萍), Hongfei Du (杜泓飞), and Wenbin He (何文斌)

Key Laboratory for Advanced Materials Processing Technology of MOE,
Department of Mechanical Engineering, Tsinghua University, Beijing 100084, China
**Corresponding author: zengp@mail.tsinghua.edu.cn*

Received January 4, 2012; accepted February 20, 2012; posted online May 16, 2012

Digital image correlation has become an important and effective non-contact optical full-field strain measurement technique. The strain field obtained directly by image correlation algorithm is full of noise. In this letter, we explore a novel way of actively adding small amount of Gaussian random noise to original displacement field, subsequently utilizing the well-known thin-plate spline smoothing (TPSS) technique to smooth the noised displacement field, and finally differentiating smoothed displacement field to get reliable strain field. The resultant method, named as active noise thin-plate spline smoothing (ANTPSS), outperforms the conventional TPSS and spline least-squares approximation. Moreover, ANTPSS successfully smooths the displacement filed obtained from three-point bending experiment of foam block and generates a reliable inhomogeneous strain field.

OCIS codes: 120.6650, 100.2000, 110.6150.
doi: 10.3788/COL201210.S11202.

Digital image correlation (DIC)[1−3] is an effective and easy-to-use technique which measures the surface deformation of samples and structures under consideration. In DIC, the problem of computing accurate and reliable strain field from direct correlation solutions is still being actively investigated. It is more practical to apply smoothing algorithms to displacement fields for performing strain analysis[4]. Thin-plate spline smoothing (TPSS) was one of the most effective methods which simultaneously consider the “closeness” of spline to observed data and spline “smoothness” by adding the smooth penalty to traditional spline lest-squares formulation. In 1991, Sutton *et al.*[5] proposed the finite element formulation of TPSS. Recently, Pan *et al.*[6] proposed pointwise least squares for strain field calculation. The spline least-squares approximation can also be used to smooth displacement field.

In this letter, we explore a novel way of actively adding small amount of Gaussian white-noise to original displacement field then smooth the noised field with TPSS and form the new method active noise TPSS (ANTPSS). Experiment on simulated tensile test and comparison between ANTPSS, TPSS and spline least-squares approximation show that the proposed ANTPSS gives more accurate strain field.

DIC is a well-established non-contact full-field deformation measurement technique. After the digital images of the spackled surface before and after deformation are recorded, the reference subset and deformed subset on two images could be mathematically compared with zero-mean normalized cross-correlation criteria (ZNCC)[7] as

$$C(\vec{p})=1-\sum_{x=-M}^{M}\sum_{y=-M}^{M}[f(x,\,y)-f_m]\times[g(x',\,y')-g_m]\Big/ \left\{\sqrt{\sum_{x=-M}^{M}\sum_{y=-M}^{M}[f(x,\,y)-f_m]^2}\sqrt{\sum_{x=-M}^{M}\sum_{y=-M}^{M}[g(x',\,y')-g_m]^2}\right\}, \tag{1}$$

where $f(x,\,y)$ and $g(x',\,y')$ represent the gray value of the reference and deformed subsets respectively, f_m and g_m are the average gray values of points in reference and deformed subsets of $(2M+1)\times(2M+1)$ pixels, and $\vec{p}$ is the deformation vector which describes the correspondance between coordinate $(x,\,y)$ and $(x',\,y')$. The coordinates $(x,\,y)$ of all points in reference subset after deformation could be expressed by first-order shape function. The bi-cubic spline interpolation could be used for gray value reconstruction.

To minimize the ZNCC criteria in Eq.(**??**), quasi-Newton (qN) method[3,4] was chosen to resolve the six deformation parametes in this study. Quasi-Newton method is an improvement of Newton-Raphson method, qN replaces the calculation and inversion of Hessian matrix by updating the approximation matrix with BFGS formula (Broydeb, Fletcher, Goldfarb, Shanno) as[3]

$$\begin{aligned}&\nabla\nabla\mathbf{C}(\vec{p}_{k+1})^{-1}\cong\mathbf{H}_{k+1}\\&=\mathbf{H}_k+\frac{1}{\vec{s}_k^{\mathrm{T}}\vec{y}_k}\left[\left(1+\frac{\vec{y}_k^{\mathrm{T}}\mathbf{H}_k\vec{y}_k}{\vec{s}_k^{\mathrm{T}}\vec{y}_k}\right)\vec{s}_k\vec{s}_k^{\mathrm{T}}-\mathbf{H}_k\vec{y}_k\vec{s}_k^{\mathrm{T}}-\vec{s}_k\vec{y}_k^{\mathrm{T}}\mathbf{H}_k\right],\end{aligned} \tag{2}$$

where $\mathbf{H}_{k+1}=\mathbf{H}(\vec{p}_{k+1})$ is the approximation of Hessian matrix $\nabla\nabla\mathbf{C}(\vec{p}_{k+1})^{-1}$, and $\mathbf{H}_0$ equals the identity matrix $\mathbf{I}$, $\vec{y}_k=\nabla\mathbf{C}(\vec{p}_{k+1})-\nabla\mathbf{C}(\vec{p}_k)$, $\vec{s}_k=\vec{p}_{k+1}-\vec{p}_k$. The iteration formula of qN could be written as

$$\vec{p}_{k+1}=\vec{p}_k-\tau\mathbf{H}(\vec{p}_k)\nabla\mathbf{C}(\vec{p}_k), \tag{3}$$

where $\tau>0$ is the step size, and τ could be further determined by inexact line-search method which includes the bracketing phase and finding acceptable point within bracket.

Thin-plate spline smoothing[8,9] is an spline based smoothing technique which is able to tackle observed data of any dimension. Generally, the task of TPSS is to minimize $S_\lambda(\alpha)$[9] of following form,

$$S_\lambda(\alpha) = \frac{1}{n}\sum_{i=1}^{n}[\bar{\alpha}(x_i, y_i) - \alpha(x_i, y_i)]^2$$

$$+ \lambda \int_{-\infty}^{+\infty}\int_{-\infty}^{+\infty}\sum_{i=0}^{m}\left(\begin{array}{c} m \\ i \end{array}\right)\left[\frac{\partial^m \alpha(x,y)}{\partial x^i \partial y^{m-1}}\right]^2 \mathrm{d}x\mathrm{d}y, \quad (4)$$

where λ is the parameter that controls the tradeoff between the smoothness of resultant spline $\alpha(x,\ y)$ of degree $2m$–1 and the infidelity of $\alpha(x,\ y)$ to the observed data $\beta(x,\ y)$, polynomial spline. Parameter λ can be determined by generalized cross-validation (GCV)[9].

In active noise thin-plate spline smoothing, additional Gaussian random noise $N\{0,\ \sigma[\beta(x_i,\ y_i)]\}$ is added to the original observed data $\beta(x_i,\ y_i)$ by

$$\eta(x_i,\ y_i) = \beta(x_i,\ y_i) + N\{0,\ \sigma[\beta(x_i,\ y_i)]\}. \quad (5)$$

The noise could be defined as constant deviation,

$$N\{0,\ \sigma[\beta(x_i,\ y_i)]\} = N\left(0,\ \delta\right), \quad (6)$$

or defined as magnitude dependent deviation model,

$$N\{0,\ \sigma[\beta(x_i,\ y_i)]\} = N[0,\ \delta\cdot|\beta(x_i,\ y_i)|], \quad (7)$$

where δ is a predefined active noise level. Then the TPSS is used to smooth the noised data $\eta(x_i,\ y_i)$. In DIC, $\beta(x_i,\ y_i)$ would be correlated displacement $u(x_i,\ y_i)$ and $v(x_i,\ y_i)$.

The performance of ANTPSS with two noise models on smoothing the actively noised displacement field for calculating strain field were verified on simulated tensile images. For comparison, original displacement fields were also smoothed directly with TPSS and spline least-squares approximation (SLSA). The reference image and deformed image with pre-assigned deformation configuration $\partial u/\partial x = 2\,000\ \mu\varepsilon$ were generated. The region of interest containing 1 225 (= 35×35) points and subset size of 31×31 pixels were selected. The deformed image is analyzed with qN method, and the obtained displacement field u on x direction and strain field $\partial u/\partial x$ are shown in Fig. 1.

The calculated displacement and strain fields in Fig. 1 are not very smooth, especially there is large variation in strain field since the pre-assigned value is 2 000 micro strain. In the following, the ANTPSS is used to smooth the displacement filed with different active noise level δ in two models, then the strain field is generated by differentiation. TPSS and SLSA are also adopted to smooth the original displacement filed. The precision of obtained strain field are evaluated with root mean-squares (RMS).

The strain fields and the corresponding RMS errors (in Fig. 2(d)) are shown in Fig. 2, where δ=0.01 is used in ANTPSS. As the results demonstrate that the RMS is very small (only 14.0 micro strains) for ANTPSS (in Fig. 2(c)) while SLSA (in Fig. 2(a)) and TPSS (in Fig. 2(b)) give rough strain field, the RMS error for TPSS is very large (124.7 micro strain). Compared with TPSS, SLSA produces smoother and better strain field, with RMS error equals 87.5 micro strains.

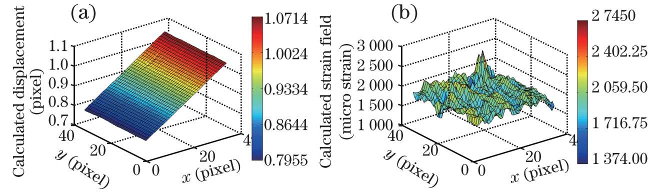

Fig. 1. (a) Calculated displacement field and (b) strain field by qN.

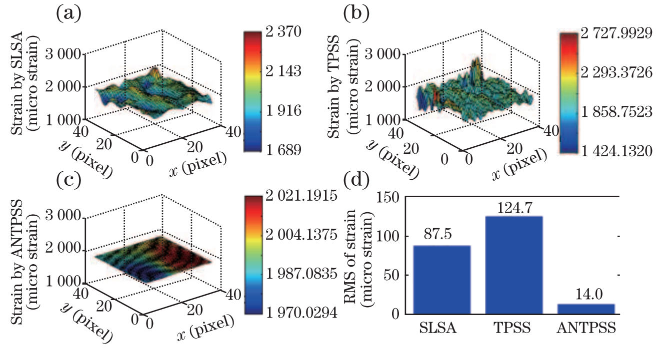

Fig. 2. Strain field by (a) SLSA, (b) TPSS, (c) ANTPSS, and (d) RMS error of stain by using these methods (δ=0.01).

To investigate the effect of noise level parameter δ on the strain field, we set δ to ten different values (δ=0, 0.001, 0.005, 0.01, 0.02, 0.05, 0.08, 0.1, 0.5, and 1), for each value, ANTPSS is run ten times, so there are 100 runs of ANTPSS. The mean RMS and standard deviation of RMS obtained with different δ are shown in Fig. 3. The RMS error that is smaller than 50 micro strains is available by setting δ in range [0.005, 0.02]. As Fig. 3 indicates, in current simulated tensile test, the optimal δ is very close to 0.01.

Similar tests are conducted when the magnitude dependent deviation model is used. In this test, δ is set to nine different values (δ=0, 0.001, 0.005, 0.01, 0.02, 0.05, 0.08, 0.1 and 0.5). Compared with the constant deviation model, the magnitude dependent deviation model leads to larger deviation in RMS as shown in Fig. 4. For constant deviation model, a wide range of δ (from 0.005 to 0.02) could be selected with low RMS error and RMS deviation, however the range is very narrow for magnitude dependent deviation model with δ closing to 0.01. As a result, constant deviation model is more robust to δ.

Both the results in Figs. 3 and 4 show that the actively added noise (corresponding to δ>0) is positive in improving the accuracy and the consistency of strain results given that parameter δ is set properly. It is also found that, the active noise is beneficial when δ is no larger than 0.02 in above two models, while the noise turns to be harmful when δ is too large (>0.05 for instance). Generally δ could be set to 1% of average displacement for most practical measurement.

To verify the performance of ANTPSS in smoothing complex displacement field for inhomogeneous strain field calculation, a three-point bending experiment was conducted for a foam block. The noisy displacement field u and strain field u_x calculated directly by qN are shown in Figs. 5(a) and (b). Then ANTPSS was used to smooth u and then u_x was com-

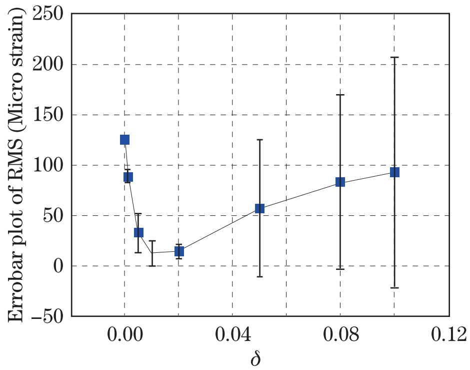

Fig. 3. Mean RMS and standard deviation of RMS obtained with different δ for the constant deviation model.

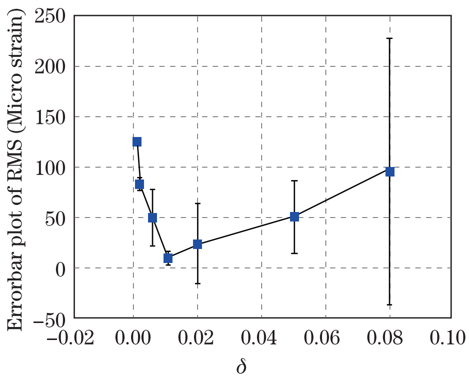

Fig. 4. Mean RMS and standard deviation of RMS obtained with different δ for the magnitude dependent deviation model.

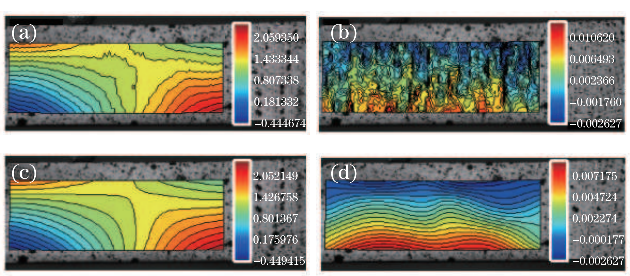

Fig. 5. Comparison between displacement field u/pixel (a), strain field u_x/ε (b) calculated by qN and smoothed u/pixel (c), u_x/ε (d) by ANTPSS.

puted by differentiation, and results are shown in Figs. 5(c) and (d) respectively. As recommended, in ANTPSS δ is set to 1% of average u field. Results show that ANTPSS could dramatically decrease the noise in u and obtain reliable strain field.

In conclusion, the active noise thin-plate spline smooth (ANTPSS) method with two Gaussian noise models are proposed to smooth the displacement field for strain measurement in digital image correlation. Experiment on simulated tensile images shows that, the root mean-squares error of resultant strain field by ANTPSS is smaller than that by original TPSS and spline least-squares approximation. Compared with magnitude dependent deviation model, ANTPSS with constant deviation model is less sensitive to setting of active noise level δ. Generally δ could be set to 1% of average displacement for most practical measurement. The proposed ANTPSS method was used to smooth the noisy displacement field obtained in the three-point bending experiment of foam block, and it generated a reliable inhomogeneous strain field. Thus, ANTPSS is a simple and effective displacement smoothing method for DIC.

The work was supported by the National Natural Science Foundation of China (Nos. 51175293 and 10972114).

References

1. M. A. Sutton, M. Cheng, W. H. Peters, Y. J. Chao, and S. R. McNeill, Image Vision Comput. **4,** 143 (1986).
2. C. Tang, M. Liu, H. Yan, G. Zhang, and Z. Chen, Chin. Opt. Lett. **2,** 574 (2004).
3. J. Zhao, P. Zeng, L. Lei, and Y. Ma, Opt. Laser Eng. **50,** 473 (2012).
4. C. Wang, J. Deng, G. A. Ateshian, and C. T. Hung, J. Biomech. Eng. **124,** 557 (2002).
5. M. A. Sutton, J. L. Turner, H. A. Bruck, and T. A. Chae, Exp. Mech. **31,** 168 (1991).
6. B. Pan, A. Asundi, H. Xie, and J. Gao, Opt. Laser Eng. **47,** 865 (2009).
7. B. Pan, H. Xie, and Z. Wang, Appl. Opt. **49,** 5501 (2010).
8. P. Craven and G. Wahba, Numer. Math. **31,** 377 (1978).
9. D. M. Bates, M. J. Lindstrom, G. Wahba, and B. S. Yandell, Commun. Statist. Simul. Comput. **16,** 263 (1987).